

Excitation Energies from Spin-Restricted Ensemble-Referenced Kohn–Sham Method: A State-Average Approach[†]

Andranik Kazaryan, Jeroen Heuver, and Michael Filatov*

Theoretical Chemistry, Zernike Institute for Advanced Materials, University of Groningen, Nijenborgh 4, 9747 AG Groningen, The Netherlands

Received: April 18, 2008

A time-independent density functional approach to the calculation of excitation energies from the ground states of molecules typified by the strong nondynamic electron correlation is suggested. The new method is based on the use of the spin-restricted ensemble-referenced Kohn–Sham formalism [Filatov, M.; Shaik, S. *Chem. Phys. Lett.* **1999**, *304*, 429] for the calculation of the ground state. In the new method, the average energy of the ground state and a state created by a single excitation thereof is minimized with respect to the Kohn–Sham orbitals and their fractional occupation numbers. The lowest singlet excitation energies obtained with the help of the new formalism for a number of model systems, such as the hydrogen molecule with stretched bond, twisted ethylene, and twisted hexa-1,3,5-triene, are compared with the results of the time-dependent density functional theory, with the results of ab initio CASSCF/CASPT2 calculations, and with the experimental data. Applicability of the new method to the description of photochemical reactions is discussed.

1. Introduction

Density functional theory (DFT)^{1–3} has become an important tool in studying the ground states of atoms and molecules. Within the framework of DFT, the excited states are commonly accessed via the use of the time-dependent formalism, TDDFT.⁴ Currently, this formalism is formulated for the nondegenerate ground states, which can be described within the single-reference Kohn–Sham approach. For molecules with the closed electronic shells, this description is sufficiently accurate and TDDFT is capable of yielding lowest excitation energies rivaling in accuracy the results from high-level wave function ab initio methods.

However, the description of molecules typified by the strong nondynamic electron correlation, such as biradicals in the low-spin states or molecules with dissociating bonds, requires the use of methods that go beyond the standard paradigm in the Kohn–Sham DFT and include the nondynamic electron correlation explicitly into consideration.^{5–10} Typically, the strong nondynamic correlation in molecules results from the (near) degeneracy of a few electronic configurations, which is often accompanied by the orbital (near) degeneracy. When an orbital (near) degeneracy is encountered in the ground state of molecule, the standard TDDFT description may break down due to the occurrence of near zero orbital energy differences in the TDDFT equations. The situations where the near degeneracy occurs can be met in molecules with dissociating bonds; well-known examples are the dissociating hydrogen molecule, where the (σ)² and the (σ^*)² configurations become near degenerate at large internuclear separations, and the double bond breaking in ethylene along the C=C twisting mode, where the (π)² and (π^*)² configurations become strictly degenerate at 90° of twist.^{11–13}

In wave function ab initio theory, the correct treatment of molecules with the strong nondynamic correlation is achieved with the use of the multireference methods, where the wave

function is approximated by a superposition of several Slater determinants (or symmetry adapted configuration-state functions) with nearly equal coefficients.¹⁴ Within DFT, one often employs the symmetry-broken spin-unrestricted method (similar to the spin-unrestricted Hartree–Fock theory)¹⁵ for the description of nondynamic correlation resulting from near degeneracy. The use of this approach, however, leads to highly spin-contaminated solutions that cannot be unambiguously assigned to specific symmetry species. An alternative approach to the nondynamic correlation within the framework of DFT is based on the use of weighted sums (ensembles) of several single-determinant Kohn–Sham configurations that are restricted to possess the correct spin and spatial symmetry.^{16–27} In the latter approach, the weighting factors in the ensembles can either be determined by the symmetry requirements, which leads to the so-called spin-restricted open-shell Kohn–Sham (ROKS) method,^{18–21} or be variationally obtained from the energy minimization as is done in the spin-restricted ensemble-referenced Kohn–Sham (REKS) method.^{22–27} It has been previously established that the former method is capable of providing the correct description of the atomic and molecular multiplet states²⁰ and the latter method describes accurately the low-spin ground states of biradicals,^{22–24} the magnetic coupling in metal complexes^{25–27} and the bond dissociation in molecules.^{22,24}

The ROKS and REKS methods are strictly applicable to the ground states (or to the lowest energy states in the given symmetry class) of molecules where mapping between the density and the potential is justified by the Hohenberg–Kohn theorems.¹ A direct optimization of the excited-state energy with respect to the excited-state density within the framework of DFT is, however, questionable²⁸ and may lead to certain artifacts in practical calculations.^{29,30} In developing a time-independent density functional theory for excited states, one has to include the ground-state density into consideration.^{31–33}

In the present work, we suggest a time-independent method to the calculation of excited states in DFT which is based on the ensemble approach. Within the ensemble approach to DFT,^{34,35} the variational principle can be applied strictly to the

[†] Part of the “Sason S. Shaik Festschrift”.

* Corresponding author. E-mail: m.filatov@rug.nl.

optimization of energies of ensembles of N lowest states of the interacting Hamiltonian as well as to ensembles of fractionally occupied and unequally weighted states.^{36,37} Thus the aforementioned difficulties with the direct optimization of the excited-state energy in DFT are avoided. For obtaining the excited-state energy, we suggest to optimize variationally a weighted sum of the energies of the ground state described by the REKS method and of the excited state described by the ROKS method. The KS orbitals obtained in this variational procedure are used to calculate the ground and the excited-state energies with the REKS and ROKS methods, respectively. Because the outlined computational approach bears a similarity with the state-average (SA) method in multireference wave function ab initio theory, the new approach is dubbed SA-REKS.

In practical implementation of the SA-REKS method, the ground singlet-state energy is combined with the energy of the lowest excited singlet state which can be obtained by a single electronic excitation from the ground state. Thus, this method can be used for theoretical modeling of photoexcitation processes^{12,13,38} in systems where the standard DFT/TDDFT methods may be not applicable because of the presence of near degeneracy effects in the ground state.^{39–43} In the following section, the SA-REKS formalism will be described and it will be applied to the calculation of the ground and excited-state energies in a number of model systems in section 3. The excitation energies and the profiles of the excited-state potential energy surface obtained in the SA-REKS calculations will be compared with the experimental data, with the results of TDDFT calculations and with the results of multireference wave function ab initio calculations carried out at the CASSCF/CASPT2 level.^{44,45}

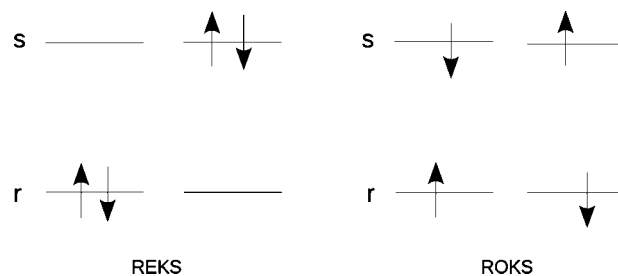
2. Method of Calculation

Let us consider a system in the singlet state with two near degenerate electronic configurations, $(\dots\varphi_r^2\varphi_s^0)$ and $(\dots\varphi_r^0\varphi_s^2)$.^{11–13,38} Restricting the description to the active orbitals φ_r and φ_s only, the configurations shown in Scheme 1 can be constructed within wave function theory. Solutions of the Schrödinger equation in the space of these configurations will generally be given by superpositions of all four configurations. However, if the orbitals φ_r and φ_s are optimized by a suitable unitary transformation which mixes φ_r and φ_s leaving them orthonormal, then the exact solutions for the two-electron two-orbital model system can be represented as in eq 1,³⁸

$$\begin{aligned}\Psi_{S_0} &= \lambda|\varphi_r\bar{\varphi}_r\rangle - \sqrt{1-\lambda^2}|\varphi_s\bar{\varphi}_s\rangle \\ \Psi_{S_1} &= \frac{1}{\sqrt{2}}(|\varphi_r\bar{\varphi}_s\rangle + |\varphi_s\bar{\varphi}_r\rangle) \\ \Psi_{S_2} &= \sqrt{1-\lambda^2}|\varphi_r\bar{\varphi}_r\rangle + \lambda|\varphi_s\bar{\varphi}_s\rangle \\ \Psi_{T_0} &= \frac{1}{\sqrt{2}}(|\varphi_r\bar{\varphi}_s\rangle - |\varphi_s\bar{\varphi}_r\rangle)\end{aligned}\quad (1)$$

where the Slater determinants $|\varphi_r\bar{\varphi}_s\rangle$ are properly normalized and it is assumed that the determinant $|\varphi_r\bar{\varphi}_r\rangle$ possesses the lowest expectation value of the Hamiltonian. Note that, as a consequence of the orbital optimization, there will be no mixing between the Ψ_{S_0} and Ψ_{S_1} functions. Thus, within the two-electron–two-orbital model, the ground-state wave function is given by Ψ_{S_0} . The Ψ_{S_1} wave function represents the state created by a single excitation from the ground state. It is these two states, Ψ_{S_0} and Ψ_{S_1} , that are targeted in the suggested density functional scheme.

SCHEME 1: Electronic Configurations in Two-Electron–Two-Orbital Model^a



^a Labels belong to the configurations employed in the REKS and in ROKS methods.

In the many-electron case, the aforementioned two-electron–two-orbital model is only an approximation that serves to illustrate the basic ideas underlying the method suggested in this work. When the two configurations, $(\dots\varphi_r^2\varphi_s^0)$ and $(\dots\varphi_r^0\varphi_s^2)$, are nearly degenerate; i.e., they correspond to the nearly degenerate expectation values of the Hamiltonian, the standard single-reference density functional description breaks down.^{5,6} In DFT, such a situation can be rigorously treated with the help of ensemble approach,^{5,6} the foundations of which have been developed in works of Lieb³⁵ and Englisch and Englisch.⁴⁶ It has been proved^{35,46} that any physical density can be represented by a weighted sum (ensemble) of densities of several states as in eq 2.

$$\rho(\mathbf{r}) = \sum_L w_L \rho_L(\mathbf{r}) \quad (2)$$

Within the Kohn–Sham approach,² the ensemble representation translates to the fractional occupation numbers of the Kohn–Sham orbitals as in eq 3,

$$\rho(\mathbf{r}) = \sum_k n_k |\varphi_k(\mathbf{r})|^2 \quad (3)$$

where the occupation numbers n_k vary between 0 and 2.

The general practical implementation of the ensemble approach to DFT is impeded by the absence of generally applicable density functionals that conform to the ensemble densities. However, for a number of situations, a representation of the energy of a strongly correlated state in terms of the Kohn–Sham orbitals and their fractional occupation numbers has been developed on the basis of the rigorous ensemble DFT combined with certain ideas from wave function theory.^{19,22} Thus, the ground singlet state of a strongly correlated system, which results from the near degeneracy of two leading configurations, can be described with the help of the REKS(2,2) method, where the nomenclature developed for the complete active space self-consistent field (CASSCF) methods is adopted. In the REKS(2,2) (two active electrons in two active orbitals) method, the density is represented as an ensemble average over densities of two configurations, $(\dots\varphi_r^2\varphi_s^0)$ and $(\dots\varphi_r^0\varphi_s^2)$, where $\varphi_r(\mathbf{r})$ and $\varphi_s(\mathbf{r})$ can be the HOMO and the LUMO in the conventional single determinant KS calculation. The inactive core Kohn–Sham orbitals are occupied with 2 electrons each, and the ground-state density is given as in eq 4.

$$\rho^{\text{REKS}}(\mathbf{r}) = \sum_{i^2}^{\text{core}} 2|\varphi_i(\mathbf{r})|^2 + n_r |\varphi_r(\mathbf{r})|^2 + n_s |\varphi_s(\mathbf{r})|^2$$

$$0 \leq n_r, n_s \leq 2; n_r + n_s = 2 \quad (4)$$

The total ground-state energy for a state with two fractionally occupied Kohn–Sham orbitals is represented as a weighted sum

of the Kohn–Sham energies of the individual configurations $E^{\text{KS}}(\dots\varphi_r^2\varphi_s^0)$ and $E^{\text{KS}}(\dots\varphi_r^0\varphi_s^2)$ and a coupling term that is expressed as a linear combination of the Kohn–Sham energies of the singly excited configurations generated within the same (2, 2) active space, see eq 5.²²

$$E^{\text{REKS}} = \frac{n_r}{2}E^{\text{KS}}(\dots\varphi_r^0\varphi_s^2) + \frac{n_s}{2}E^{\text{KS}}(\dots\varphi_r^2\varphi_s^0) + f(n_r, n_s) \left[E^{\text{KS}}(\dots\varphi_r\varphi_s) - \frac{1}{2}E^{\text{KS}}(\dots\varphi_r\bar{\varphi}_s) - \frac{1}{2}E^{\text{KS}}(\dots\bar{\varphi}_r\varphi_s) \right] \quad (5)$$

In eq 5, the factor $f(n_r, n_s)$ is given by eq 6,²⁷

$$f(n_r, n_s) = (n_r n_s)^{1-(1/2)[(n_r n_s + \delta)/(1 + \delta)]} \quad \delta = 0.4 \quad (6)$$

which interpolates between the regimes of strong nondynamic correlation, where $n_r \approx n_s \approx 1$, and the “normal” state with $n_r = 2$ and $n_s = 0$. The use of eq 6 helps to eliminate the double counting of the correlation energy as evidenced by a comparison of the REKS(2,2) total energies and the usual single-reference Kohn–Sham energies for “normal” states.^{22,27}

In the REKS calculation, the Kohn–Sham orbitals and the fractional occupation numbers of the active orbitals are obtained variationally via the energy minimization under the orbital orthogonality constraints.^{19,20,22} The fractional occupation numbers in REKS are analogous to the natural orbital occupation numbers in conventional wave function multireference methods. Thus, one can analyze the REKS density and energy in similar terms as in conventional wave function theory.

Although the REKS method is formulated for the ground state only, the energy of the open-shell singlet excited state S_1 in eq 1 can be calculated nonvariationally using the REKS optimized orbitals. For this purpose, the ROKS method^{16–21} can be employed, in which the energy is given by eq 7.

$$E^{\text{ROKS}-S_1} = E^{\text{KS}}(\dots\varphi_r\bar{\varphi}_s) + E^{\text{KS}}(\dots\bar{\varphi}_r\varphi_s) - E^{\text{KS}}(\dots\varphi_r\varphi_s) \quad (7)$$

Such a nonvariational calculation yields an upper limit to the energy of the excited S_1 state in the two-electron–two-orbital model. Although, in wave function theory, a better estimate for the excited-state energy can be obtained from the variational optimization of the orbitals in the S_1 state, such an optimization is not theoretically justified in the context of DFT.^{28–30} To obtain a better approximation to the $S_1 \leftarrow S_0$ excitation energy, one can employ the ensemble formalism and optimize the Kohn–Sham orbitals with respect to a weighted sum of the ground S_0 state and the singly excited S_1 state as in eq 1,

$$E^{\text{SA-REKS}} = C_1 E^{\text{REKS}-S_0} + C_2 E^{\text{ROKS}-S_1} \quad (8)$$

where the (positive definite) coefficients C_1 and C_2 sum up to unity. As has been pointed out in the Introduction, the variational principle is valid for such an ensemble within the context of DFT.^{36,37} The energy (8) is optimized with respect to both the Kohn–Sham orbitals and the fractional occupation numbers. The Kohn–Sham orbitals obtained from this variational procedure can be used to calculate the energies of the S_0 (eq 5) and S_1 (eq 7) states. Note that, when calculating the S_0 energy according to eq 5, the fractional occupation numbers of the active orbitals are optimized, however the orbitals are kept frozen. Because the outlined procedure bears a similarity with the state-average (SA) approach in conventional wave function theory, it is suggested to dub the new procedure as SA-REKS.

The described computational procedure has been implemented in the COLOGNE08 code,⁴⁷ with the help of which the ground-state REKS calculations and the SA-REKS calculations have

been carried out. In all density functional calculations, the 6-311G+(3df,2p) basis set⁴⁸ was employed unless noted otherwise. DFT calculations were carried out with the use of B3LYP⁴⁹ and BH&HLYP^{50,51} density functionals. CASSCF/CASPT2^{44,45} calculations have been carried out with the help of the MOLCAS 7 code.⁵² In the following section, the results of the SA-REKS calculations will be presented and compared with the excitation energies obtained in TDDFT calculations and in CASSCF/CASPT2 calculations.

3. Results

The formalism described in the preceding section has been tested in the calculations of the lowest excited singlet states for a number of model systems. The benchmark set comprises the following molecules: hydrogen molecule H_2 , ethylene C_2H_4 , and hexa-1,3,5-triene C_6H_8 , which is often used in modeling photoisomerization of large unsaturated molecules.^{53–55} The results of the SA-REKS calculations are compared with the excitation energies calculated with the use of time-dependent density functional theory and with high level multireference ab initio methods and with the available experimental data.

3.1. Excitation Energy in H_2 along the Bond Stretching Mode. A hydrogen molecule at a stretched interatomic distance is often employed as a prototypical system to study the effect of nondynamic electron correlation.^{40,56,57} Failure of single-reference spin-restricted wave function ab initio and density functional methods to describe the potential energy curve of dissociating H_2 is well documented.^{40,56} Beyond the Coulson–Fischer point (ca. 2.75 bohr for R_{H-H})⁵⁸ the single-reference description breaks down and the dissociation curve produced by single-reference spin-restricted methods goes to a higher energy than the energy of two noninteracting atoms.

The excitation energy to the lowest $^1\Sigma_u^+$ state of hydrogen molecule as a function of internuclear distance has been previously calculated with the use of TDDFT.⁵⁷ In the present work, the REKS method is applied to this system besides the TDDFT approach, which is used for comparison. The potential energy curves for the ground $^1\Sigma_g^+$ and excited $^1\Sigma_u^+$ states of H_2 are shown in Figure 1 and the $^1\Sigma_u^+ \leftarrow ^1\Sigma_g^+$ excitation energy is shown in Figure 2 as a function of distance. At short internuclear distances (less than 2 bohr), the excited-state curves obtained in TD-B3LYP and in TD-BH&HLYP calculations match reasonably well the shape of the exact curve obtained from the calculations of Kołos and Wolniewicz,^{59,60} which are used as a reference in this work. However, beyond the Coulson–Fischer point, the curves obtained with TDDFT begin to deviate rapidly from the exact behavior and at large separations a negative excitation energy is obtained, which indicates the breakdown of the spin-restricted single-reference description of the reference ground state.⁵⁷

The wrong behavior of the excitation energy from TDDFT on H–H distance is clearly visible in Figure 2. The exact excitation energy has a minimum at $R_{H-H} = 4.1$ bohr. The TD-B3LYP and TD-BH&HLYP excitation curves do not show any minimum and go monotonously down as the internuclear distance increases. Precisely that behavior of the TDDFT method has been previously documented in ref 57.

The ground $^1\Sigma_g^+$ and excited $^1\Sigma_u^+$ states potential energy curves obtained with REKS and state-average REKS methods using the B3LYP and BH&HLYP density functionals are shown in Figure 1. REKS calculations with both density functionals reproduce nicely the exact potential energy curve for the ground state. B3LYP functional shows slightly better performance which can be attributed to the fact that this functional was

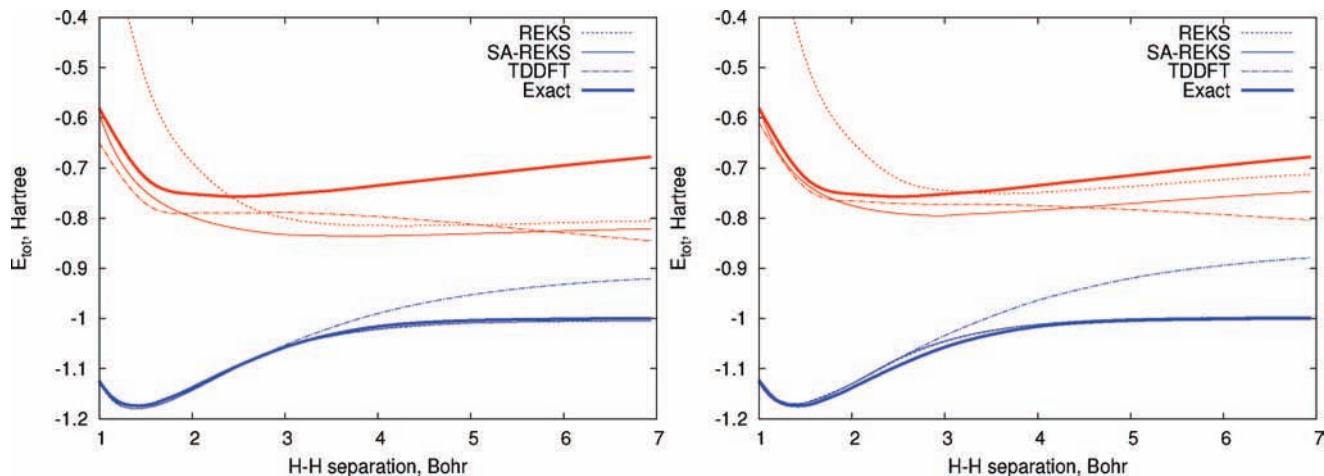


Figure 1. Total energy of H₂ at varying internuclear distance in ${}^1\Sigma_g^+$ (blue) and in ${}^1\Sigma_u^+$ (red) states. Calculations were performed with B3LYP (left panel) and BH&HLYP (right panel) functionals. Exact curves are from refs 59 and 60.

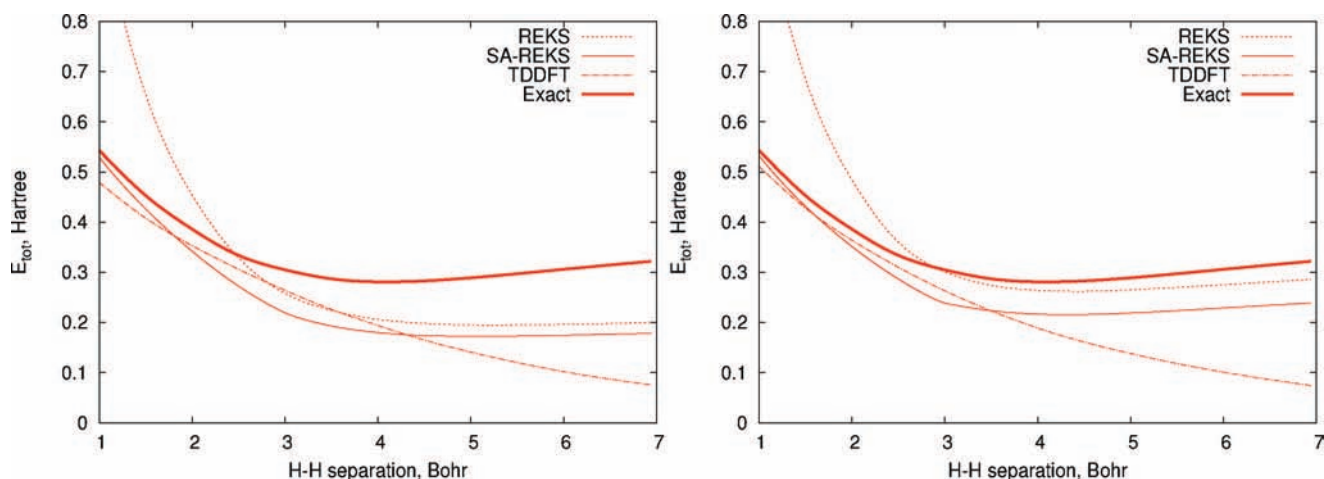


Figure 2. Excitation energy ${}^1\Sigma_u^+ \leftarrow {}^1\Sigma_g^+$ of the hydrogen molecule as a function of distance. Calculations were performed with B3LYP (left plot) and BH&HLYP (right plot) functionals. Exact curve is from ref 60.

empirically optimized to accurately reproduce thermochemical parameters of molecules in ground states. The ground-state energies obtained in the SA-REKS calculations are within 1 kcal/mol from the values obtained in the state-specific REKS calculations.

For the ${}^1\Sigma_u^+ \leftarrow {}^1\Sigma_g^+$ excitation energy, the difference between the state-average and state-specific REKS calculations is more pronounced. Although, at large interatomic distances, both methods (state-average and state-specific) agree reasonably well, there is a marked difference at short H–H separations. Near the equilibrium bond length, the state-specific REKS method converges to the usual closed-shell single-reference solution with the bonding $1\sigma_g$ Kohn–Sham orbital doubly occupied and the antibonding $1\sigma_u$ orbital empty. Because the ground-state energy in such a case does not depend on the shape of the antibonding orbital, this orbital does not attain a shape suitable for good description of the ${}^1\Sigma_u^+$ excited state, where both orbitals, $1\sigma_g$ and $1\sigma_u$, are singly occupied. In the state-average calculation, both orbitals are optimized in such a way so as to minimize the weighted average of the ground and excited-state energies (8) with $S_0 = {}^1\Sigma_g^+$ and $S_1 = {}^1\Sigma_u^+$.

The state-average optimization of REKS orbitals results in a much better agreement of the excited ${}^1\Sigma_u^+$ state energy with the exact energy, as evidenced by Figures 1 and 2. The discrepancy between the REKS excitation energy and the exact energy at short H–H distances is considerably improved. The excitation

energy curve shows a shallow minimum at 5.1 bohr from SA-REB3LYP calculation and at 4.3 bohr from SA-REBH&HLYP calculation which is to be compared with the exact minimum at 4.1 bohr (see Figure 2). The magnitude of the ${}^1\Sigma_u^+ \leftarrow {}^1\Sigma_g^+$ excitation energy is somewhat underestimated at the large H–H distances. This can be interpreted as originating from over-stabilization of ionic states with respect to covalent states by approximate density functionals. Note that the ${}^1\Sigma_u^+$ excited state of H₂ has an ionic character, whereas the ${}^1\Sigma_g^+$ ground state possesses a covalent character. The over-stabilization of ionic states can be traced back to the effect of electron self-interaction error in approximate density functionals,^{24,61,62} which leads to somewhat too diffuse occupied KS orbitals. As more self-interaction error free Hartree–Fock exchange energy is mixed into a hybrid HF/DFT functional, such as BH&HLYP, the overall effect of such an over-stabilization subsides and the excitation energy to the ionic ${}^1\Sigma_u^+$ state obtained in REKS calculations improves (see Figure 2).

The state-average REKS calculations reported in Figures 1 and 2 are carried out with the use of equal weighting factors in eq 8. With a different choice of the weighting factors C_1 and $C_2 = 1 - C_1$, a slightly different value of the excitation energy can be obtained. Figure 3 shows the dependence of the ${}^1\Sigma_u^+ \leftarrow {}^1\Sigma_g^+$ excitation energy obtained in state-average REKS calculations on the choice of weighting factors. Obviously, with the $C_1 = 1$ the results of a state-specific calculation are reproduced.

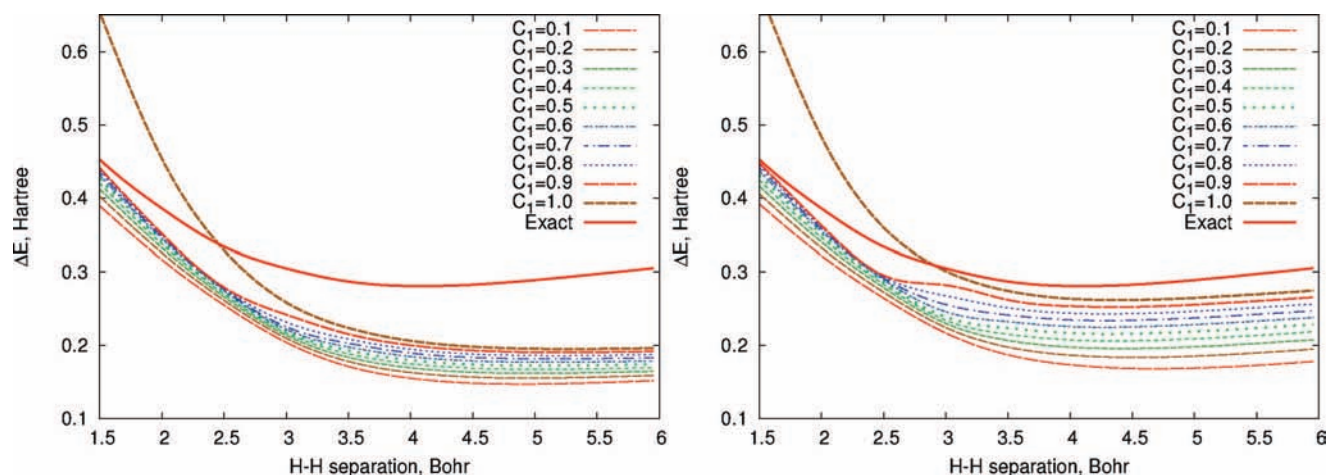


Figure 3. Excitation energy of H_2 (see caption to Figure 2) calculated with SA-REKS method with the use of varying weighting factors C_1 and C_2 (see eq 8). Exact curve is from ref 60.

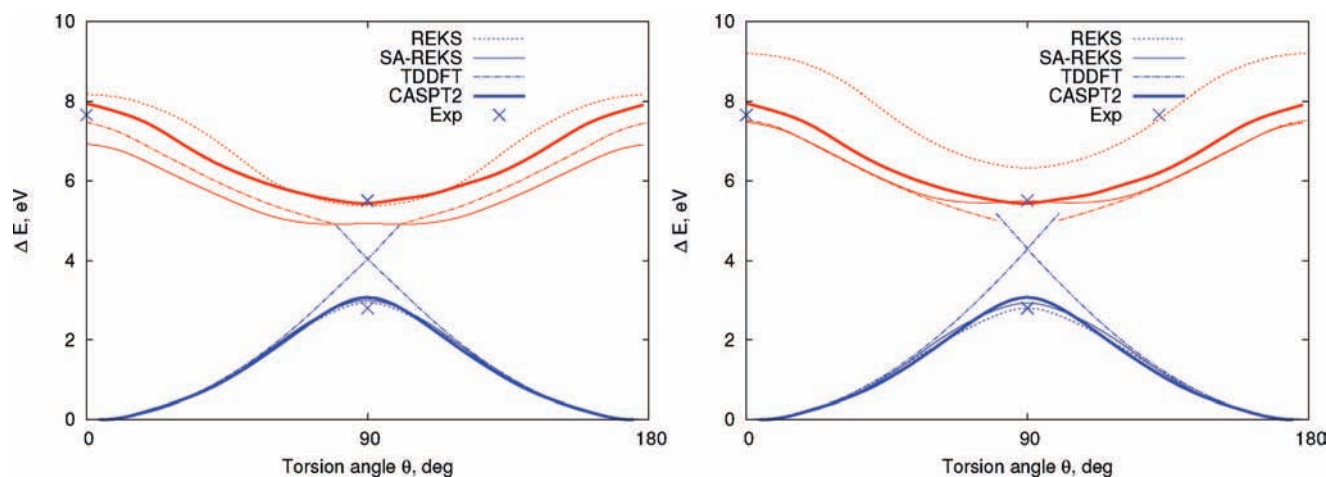


Figure 4. Potential energy profiles of ethylene along double bond twisting mode. Blue curves correspond to the 1^1A_g ground state and red curves to the 1^1B_u excited state. TDDFT, REKS and SA-REKS calculations were performed with B3LYP (left) and BH&HLYP (right) exchange–correlation functionals. The experimental vertical excitation energy is from ref 66 and adiabatic excitation energy (at 90°) is from ref 65. The rotation barrier height is from ref 64.

However, with C_1 varying between 0.1 and 0.9 the excitation energy curves bundle within a narrow range around the curve corresponding to $C_1 = 0.5$. Such that the choice of equal weighting factors in eq 8 corresponds to a median value of the excitation energy, which can be obtained in state-average calculation with varying weighting factors. This choice of the weighting factors, $C_1 = C_2 = 0.5$, in state-average REKS calculations is adopted throughout this work.

3.2. Ethylene. Twisting about the double bond in ethylene represents another widely used example where strong nondynamic correlation occurs in the ground state of the molecule.^{12,13,38} In the ground 1^1A_g state, ethylene attains a planar conformation (D_{2h} point group) with two carbon atoms bound by a double bond. Along the twisting mode, as the twisting angle approaches 90° the energy gap between the π and π^* orbitals of the double bond decreases and the nondynamic correlation due to near degeneracy of the $(\dots)(\pi)^2$ and $(\dots)(\pi^*)^2$ configurations sets in. At a 90° twist, the two configurations are strictly degenerate due to symmetry in the D_{2d} point group and both orbitals, π and π^* , are singly occupied.^{12,13,38}

The π -bond breaking along the twisting mode in ethylene cannot be described within a single-reference approach, such as the usual spin-restricted Kohn–Sham approach. This failure is well documented in the literature^{22,63} and is illustrated in Figure 4, where the results of the spin-restricted KS and TDDFT

calculations are shown with dashed-dotted lines. In Figure 4, it is clearly seen that, in the single reference description, the ground-state energy even after 90° of twist corresponds to a doubly occupied π orbital and does not smoothly switch to the $(\dots)(\pi^*)^2$ configuration.

The 1^1B_{1u} excited state of the planar C_2H_4 is well described within the TDDFT approach with the use of both density functionals, B3LYP and BH&HLYP. The excitation energy is somewhat underestimated with the use of the B3LYP functional whereas the TD-BH&HLYP energy is in fairly good agreement with that from the experiment. The TD-BH&HLYP excitation energy is in markedly better agreement with the experimental value than the (6,4)CASPT2 energy, which is overestimated by ca. 0.3 eV. In all the calculations, TDDFT and CASSCF/CASPT2, the geometry optimized with the REB3LYP/6-311G+(3df,2p) method along the minimal energy path on the ground-state potential energy surface was employed. For the planar ethylene, this geometry is identical to the geometry obtained with the usual single reference B3LYP method.

With the use of the RE-B3LYP/6-311G+(3df,2p) molecular geometry, the excitation energy to the lowest 1^1B_1 (D_2 point group) state was calculated within the TDDFT approach. At small twisting angles, the TDDFT excited-state PES follows more or less accurately the profile of the CASPT2 PES. However, beyond ca. 70° of twist, the TDDFT excited-state

TABLE 1: Total Energies of the Ground ${}^1\Sigma_g^+$ and Excited ${}^1\Sigma_u^+$ States of H_2 and the Corresponding Excitation Energies As Obtained with Different Density Functional Methods

functional	state	R_{H-H} , bohr	TD-DFT	REKS	SA-REKS ^a	exact ^{59,60}	
B3LYP	${}^1\Sigma_g^+$	1	-1.1291	-1.1323	-1.1219	-1.1245	
		3	-1.0532	-1.0583	-1.0522	-1.0573	
		7	-0.9197	-1.0047	-0.9994	-1.0002	
	${}^1\Sigma_u^+$	1	-0.6497	-0.6497	-0.1506	-0.5927	-0.5813
		3	-0.7891	-0.7999	-0.8329	-0.7525	
		7	-0.8461	-0.8050	-0.8210	-0.6772	
		${}^1\Sigma_u^+ \leftarrow {}^1\Sigma_g^+$	1	0.4794	0.9817	0.5292	0.5432
	BH&HLYP	${}^1\Sigma_g^+$	3	0.2640	0.2584	0.2193	0.3048
			7	0.0736	0.1997	0.1784	0.3230
			1	-1.1206	-1.1206	-1.1132	-1.1245
${}^1\Sigma_u^+$		3	-1.0342	-1.0462	-1.0336	-1.0573	
		7	-0.8775	-0.9974	-0.9858	-1.0002	
		1	-0.6099	-0.0973	-0.5812	-0.5813	
		3	-0.7716	-0.7452	-0.7950	-0.7525	
${}^1\Sigma_u^+ \leftarrow {}^1\Sigma_g^+$	7	-0.8041	-0.7116	-0.7464	-0.6772		
	1	0.5107	1.0234	0.5320	0.5432		
	3	0.2626	0.3010	0.2386	0.3048		
	7	0.0734	0.2857	0.2393	0.3230		

^a Equal weighting factors are used in the state-average calculations.

TABLE 2: $S_1 \leftarrow S_0$ Excitation Energies in Ethylene and the Barrier to Rotation in the Ground S_0 State As Obtained with Different Methods

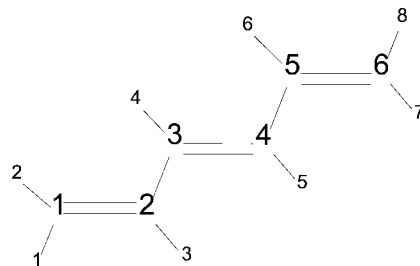
functional	torsion angle	state	SA-		TD-		exp
			REKS	REKS ^a	DFT	CASPT2	
B3LYP	0	S_0					
		S_1	8.18	6.93	7.17	7.95	7.66 ^b
	90	S_0	2.94	3.00	4.06	3.06	2.8 ^c
		S_1	5.36	4.92		5.48	5.5 ^d
BH&HLYP	0	S_0					
		S_1	9.20	7.48	7.53	7.95	7.66 ^b
	90	S_0	2.80	2.93	3.46	3.06	2.8 ^c
		S_1	6.32	5.49		5.48	5.5 ^d

^a Equal weighting factors are used in the state-average calculations. ^b From ref 66. ^c From ref 64. ^d From ref 65.

surface crosses the ground-state energy surface, which leads to the breakdown of the TDDFT calculations, thus rendering impossible to describe the excited-state PES with TDDFT in this region.

The excited-state PES along the twisting mode in ethylene is nicely described within the REKS approach as shows comparison with the (6,4)CASPT2 energies and with the available experimental data;^{64–66} see Figure 4 and Table 2. With the use of the REKS orbitals optimized for the ground state, the excitation energy in the planar conformation is overestimated in both sets of calculations, REB3LYP and REBH&HLYP. Similar to the case of H_2 at the equilibrium bond length, this is a consequence of the fact that the π^* orbital is empty in the planar ground-state electronic configurations and is not optimized during the state-specific REKS calculation.

Optimizing the REKS orbitals with respect to the average energy, $0.5E({}^1A_g) + 0.5E({}^1B_{1u})$, of the ground and excited states leads to a noticeable lowering (ca. 1 eV) of the excitation energy as obtained with the SA-REKS method. The excitation energy obtained with the SA-REBH&HLYP method is in a very good agreement with the experimental value. Interestingly, the excited-state PESs obtained with the SA-REBH&HLYP and TD-BH&HLYP methods are nearly indistinguishable at twisting angles below ca. 50° . The shape of the excited-state PES obtained in the SA-REB3LYP and SA-REBH&HLYP calculations follows the profile of the (6,4)CASPT2 PES fairly well (see Figure 4). The excited-state PES obtained with SA-REB3LYP is shifted downward by ca. 0.5–1 eV with respect

SCHEME 2: Numbering of Atoms in *trans*-1,3,5-Hexatriene

to the (6,4)CASPT2 PES. This is yet another manifestation of the effect of self-interaction error in density functional calculations. Mixing in more Hartree–Fock exchange leads to narrowing of the gap between SA-REKS and CASPT2 PESs and the SA-REBH&HLYP excited-state PES is in a much better agreement with the (6,4)CASPT2 curve. It is noteworthy that there is a very nice agreement between the SA-REBH&HLYP excitation energies and the experimental data at both planar and 90° -twisted conformations of ethylene (see Table 2).

3.3. Hexa-1,3,5-triene. Hexa-1,3,5-triene is often used as a prototype system in studying photoisomerization processes in large unsaturated molecules, such as synthetic molecular motors and biologic photosensitive molecules.^{54,55,67} In hexa-1,3,5-triene, the frontier orbitals, the highest occupied molecular orbital (HOMO) and the lowest unoccupied molecular orbital (LUMO), correspond to the bonding and the antibonding π orbitals of the central double bond; see Scheme 2. In the photoexcitation of hexa-1,3,5-triene, a HOMO–LUMO electronic transition takes place, which leads to breaking of the central C_3 – C_4 double bond. As a result, the two allyl fragments, C_1 – C_2 – C_3 and C_4 – C_5 – C_6 , can rotate freely about the C_3 – C_4 bond, which leads to isomerization of the *trans*- and *cis*-conformations. Similarly to the case of ethylene twisting and hydrogen dissociation, the correct description of the ground and excited-state potential energy surfaces of hexa-1,3,5-triene requires the inclusion of nondynamic electron correlation, because near the 90° of twist about the C_3 – C_4 bond, the configurations corresponding to the doubly occupied HOMO and the doubly occupied LUMO become nearly degenerate.

The single-reference spin-restricted DFT approach fails to describe the PES of the ground state of hexa-1,3,5-triene along

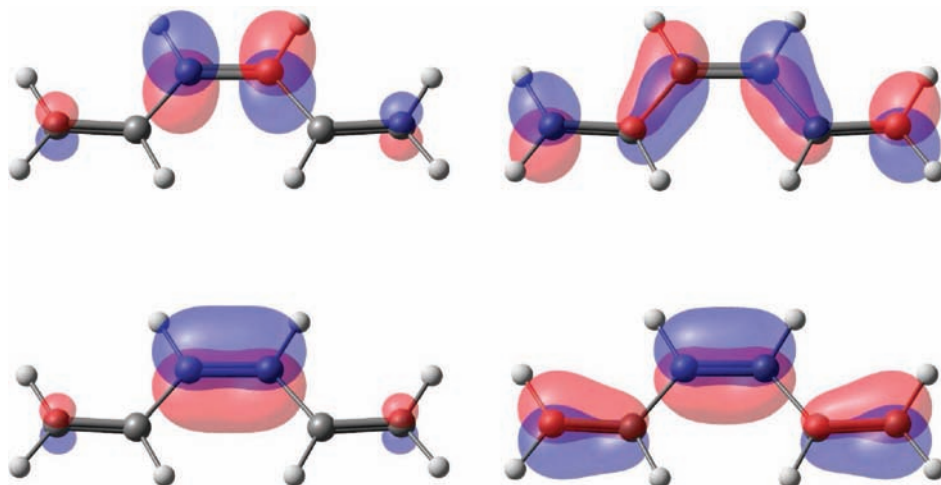


Figure 5. HOMO and LUMO orbitals of 1,3,5-*cis*-hexatriene obtained by REKS (left) and SA-REKS (right) methods.

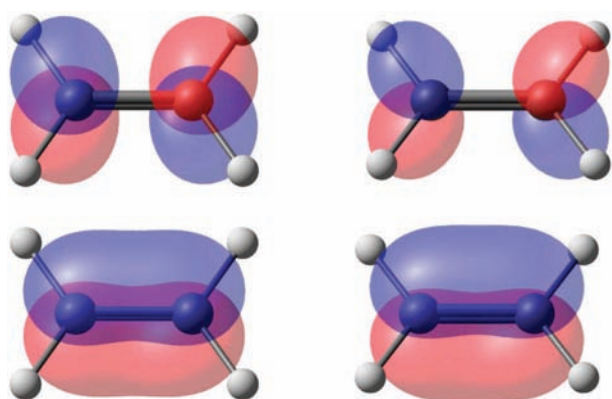


Figure 6. HOMO and LUMO orbitals of ethylene obtained by REKS (left) and SA-REKS (right) methods.

the C_3 – C_4 twisting mode. Similar to the case of ethylene, there is a cusp on the DFT PES near 90° of twist. The geometry along the minimal energy path along the C_3 – C_4 twisting mode was obtained in the REB3LYP/6-311G+(3df,2p) geometry optimization. The REKS ground-state potential energy surface is smooth and compares fairly well with the ground-state PES obtained in the (6,6)CASPT2 calculation (see Figure 7). The geometry of *trans*-hexa-1,3,5-triene is compared in Table 3 with the available experimental data,⁶⁸ and the results of the wave function ab initio calculations carried out at the second order Møller–Plesset (MP2) many-body perturbation theory level.⁶⁹ The ground-state molecular geometry of *trans*-hexa-1,3,5-triene obtained with REB3LYP/6-311G+(3df,2p) method is in a very good agreement with the MP2 geometry.

The excitation energy of the planar *trans*-hexa-1,3,5-triene calculated with TDDFT is in a fairly good agreement with the experimental datum⁷⁰ (see Table 4). Both density functionals employed, B3LYP and BH&HLYP, predict the excitation energies within 0.3 eV from the experimental figure. For small twisting angles, the profile of the excited-state PES along the minimal energy path of the C_3 – C_4 twisting obtained in the TDDFT calculations follows reasonably well the PES obtained in the (6,6)CASPT2 calculations. However, beyond ca. 50° of twist the TDDFT excited-state PES begins to deviate from the shape predicted by (6,6)CASPT2 and around ca. 80° of twist the TDDFT description of the excited-state breaks down. Beyond this twisting angle, it was not possible to obtain converged TDDFT excitation energies.

The excited-state PES obtained in the REKS calculation using the orbitals optimized for the ground state alone, shows fairly strong deviation from both the experimental excitation energy and from the (6,6)CASPT2 PES for the planar *trans*-hexa-1,3,5-triene. Similar to the case of the ground state of planar ethylene, this can be explained by the fact that the LUMO in the ground state is empty and is thus poorly optimized in the REKS calculation. When the twisting angle approaches 90° , the nondynamic correlation leads to (nearly) equal populations of the HOMO and LUMO and both orbitals are optimized in the REKS calculation equally well. Thus the part of the excited-state PES which corresponds to these twisting angles is reproduced fairly well in the state-specific REKS calculations.

Switching to the state-average REKS method brings in a considerable improvement of the excited-state PES. The excitation energy of the planar *trans*-hexa-1,3,5-triene is lowered by almost 3 eV, which brings this energy in much better agreement with the experimental and (6,6)CASPT2 energies. Such a huge energy lowering due to using the state-average approach can be explained by the difference in the shapes of frontier orbitals obtained in state-specific and state-average calculations. The HOMO and LUMO of the planar *trans*-hexa-1,3,5-triene optimized with respect to the energy of the ground state only and the orbitals optimized with respect to the average energy of the ground and excited states, $0.5E_{g.s.} + 0.5E_{e.s.}$, are shown in Figure 5. It is clearly seen that the orbitals optimized in the state-average approach are more delocalized as compared to the orbitals optimized with respect to the ground-state energy alone. This is a clear reflection of the ionic nature of the excited state of hexatriene. In comparison with ethylene, the frontier orbitals that were optimized using the two approaches are shown in Figure 6, there is much more pronounced change in the shape of the frontier orbitals with the use of the state-average approach. Indeed, in ethylene, the shape of the frontier orbitals is defined primarily by molecular symmetry and the possibilities for delocalization of the HOMO and LUMO are fairly limited. Thus the excitation energy changes by ca. 1 eV only when switching from the state-specific to the state-average method. In hexatriene, the delocalization of frontier orbitals along the terminal double bonds take place which leads to a more pronounced effect on the excitation energy. This comparison demonstrates the superiority of the state-average method over the state-specific one for the calculation of excitation energies.

The shape of the excited-state PES along the C_3 – C_4 twisting mode obtained in the SA-REB3LYP and in the SA-

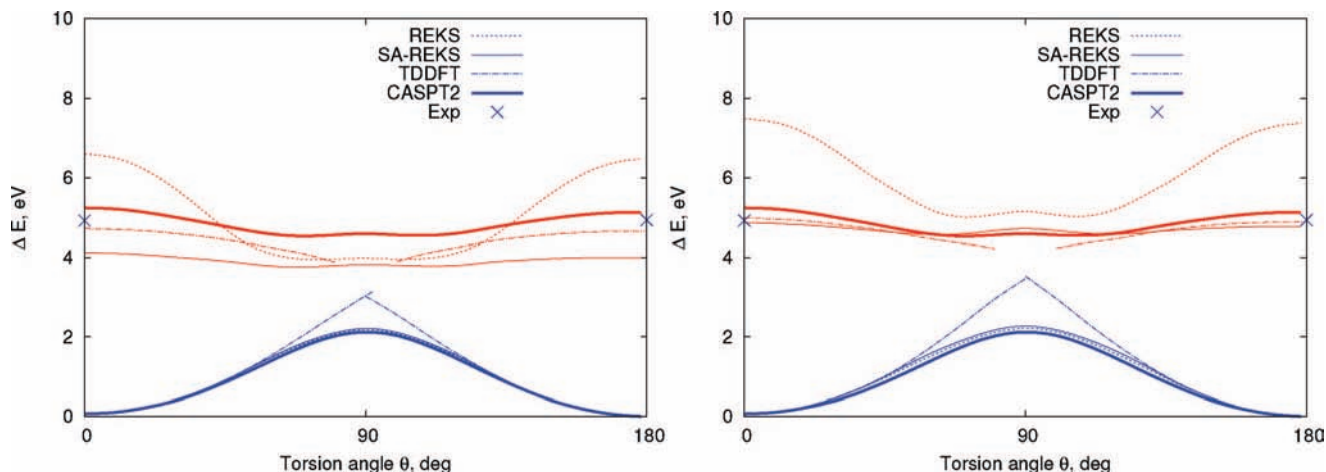


Figure 7. Potential energy profiles along torsional angle $\angle C_2C_3C_4C_5$ in hexa-1,3,5-triene. Blue curves correspond to the 1^1A ground state and red curves to the 1^1B excited state. TDDFT, REKS and SA-REKS calculations were performed with B3LYP (left) and BH&HLYP (right) exchange–correlation functionals. The experimental value is from ref 70.

TABLE 3: Geometry of *trans*-Hexa-1,3,5-triene in the Ground 1^1A_g State As Obtained with Different Methods (Atomic Labels in Scheme 2)

	REKS	MP2/cc-pVTZ [69]	exp ⁶⁸
C ₁ =C ₂	1.337	1.350	1.337
C ₂ =C ₃	1.445	1.446	1.458
C ₃ =C ₄	1.346	1.343	1.368
C ₁ =H ₂	1.083	1.082	1.104
C ₁ =H ₁	1.081	1.080	1.104
C ₂ =H ₃	1.086	1.085	1.104
C ₃ =H ₄	1.087	1.086	1.104
$\angle C_1C_2C_3$	124.489	123.678	121.7
$\angle C_2C_3C_4$	124.300	123.684	124.4
$\angle C_2C_1H_2$	121.497	120.860	120.5
$\angle C_2C_1H_1$	121.652	121.410	120.5
$\angle C_4C_3H_4$	118.944	118.966	115.0
$\angle C_3C_2H_3$	116.407	116.908	121.3

TABLE 4: Energies of $S_1 \leftarrow S_0$ Excitation and the Barrier to Rotation about the Central Double Bond in *trans*-Hexa-1,3,5-triene

functional	torsion angle (deg)	state	SA-		TD-DFT	CASPT2	exp ⁷⁰
			REKS	REKS ^a			
B3LYP	180	S ₀					
		S ₁	6.49	4.04	4.65	5.13	4.93
	90	S ₀	2.18	2.19	3.03	2.12	
		S ₁	3.98	3.93		4.59	
BH&HLYP	180	S ₀					
		S ₁	7.47	4.77	4.89	5.13	4.93
	90	S ₀	2.19	2.27	3.52	2.12	
		S ₁	5.13	4.72		4.59	

^aEqual weighting factors are used in the state-average calculations.

REBH&HLYP calculations follows the shape of the (6,6)CASPT2 PES for all twisting angles. It is interesting that, similar to the case of ethylene twisting, the SA-REBH&HLYP PES coincides with the respective TDDFT PES for small twisting angles. In this region, the nondynamic correlation is weak and the single-reference description of the ground state is sufficient. It is gratifying that, for large twisting angles, the SA-REBH&HLYP PES is nearly indistinguishable from the (6,6)CASPT2 PES. This demonstrates that, for all twisting angles, the SA-REKS method is capable of describing the ground and excited potential energy surfaces with high accuracy.

4. Conclusions

The present work was motivated by the necessity to describe the excited states of molecules in the ground states of which the strong nondynamic electron correlation is present. Diradicals in the low-spin states, molecules with partially dissociated bonds are typified by the presence of the nondynamic correlation resulting from near degeneracy of several electronic configurations.^{38,71} The correct description of the ground states of these molecules can be achieved with the use of the so-called spin-restricted ensemble-referenced Kohn–Sham (REKS) method,²² in which the nondynamic correlation is taken into account via the use of fractional occupation numbers of several frontier Kohn–Sham orbitals resulting from the ensemble averaging of a few noninteracting KS reference determinants. Previously, this approach has been successfully applied to study the ground states of various diradicaloid species^{22–27} and the present work extends its domain of applicability to the excited states.

The new method suggested in the present work is based on the use of the REKS orbitals for the calculation of the energy of an excited state which can be created by a single electronic excitation from the ground state. Such a situation is typical for photoisomerization processes,^{12,38} where a molecule in the excited singlet state undergoes a number of chemical rearrangements before relaxing into the ground singlet state. The photoexcitation results in the formation of a state in which one (or more) chemical bond is dissociated, partially or completely, and the correct theoretical description of the whole process requires the use of a method capable of taking the nondynamic correlation into account both in the ground state and in the excited state.

The energy of the open-shell singlet state can be straightforwardly calculated with the use of the so-called spin-restricted open-shell Kohn–Sham method, for the first time suggested by Ziegler, Rauk, and Baerends¹⁶ and later developed by others.^{18–21} However, if such a state is the excited state of a molecule, the direct optimization of its energy with respect to the excited-state density is questionable within the framework of Kohn–Sham DFT.^{28–33} This problem can be bypassed with the use of the KS orbitals optimized for the ground state or for an ensemble of the ground and the excited states.⁵ In the present work, we have formulated and tested a state-average version of the REKS method, in which the KS orbitals are optimized with respect to a weighted sum of the energies of the ground state and the singly excited state. The ground-state energy is

represented as in the ground-state REKS method, whereas, for the excited open-shell singlet state, the ROKS formalism is employed.

In the calculations of several model systems, which include the hydrogen molecule with stretched bond, twisting about the double bond in ethylene and twisting about the central double bond in hexa-1,3,5-triene, the applicability of the new approach to the calculation of the ground and excited-state potential energy surfaces has been tested. In comparison with the available experimental data and with the results of ab initio CASSCF/CASPT2 calculations, it has been found that the new method, SA-REKS, is capable of describing the ground and excited-state PESs with high accuracy. The excited-state PESs obtained with SA-REKS, correctly reproduce the shape predicted by the high-level ab initio method. The magnitude of the excitation energies obtained in the SA-REBH&HLYP calculations are within 0.2 eV from the experimental values. It should be noted that the TDDFT description of the excited-state PESs breaks down in the systems typified by the strong nondynamic correlation and unrealistic excitation energies result in these situations. However, in situations where the near degeneracy effects are not present, such as the ground state of planar ethylene or of planar hexa-1,3,5-triene, the TDDFT formalism yields accurate excitation energies. It is gratifying that, for these systems, the new SA-REKS method is capable of reproducing the TDDFT results. Thus, the new method describes accurately the lowest singlet excited states in both situations, when the near degeneracy effects are strong and when they are weak or absent. This method is therefore well suited for modeling of the photoisomerization processes.

References and Notes

- (1) Hohenberg, P.; Kohn, W. *Phys. Rev. B* **1964**, *136*, 864.
- (2) Kohn, W.; Sham, L. J. *Phys. Rev. A* **1965**, *140*, 1133.
- (3) Jones, R. O.; Gunnarsson, O. *Rev. Mod. Phys.* **1989**, *61*, 689.
- (4) Casida, M. In *Recent Advances in Density Functional Methods*; Chong, D. P. Ed.; World Scientific: Singapore, 1995; p 155.
- (5) Schipper, P. R. T.; Gritsenko, O. V.; Baerends, E. J. *Theor. Chem. Acc.* **1998**, *99*, 329.
- (6) Ullrich, C. A.; Kohn, W. *Phys. Rev. Lett.* **2001**, *87*, 093001.
- (7) Wu, W.; Luo, Y.; Song, L.; Shaik, S. *Phys. Chem. Chem. Phys.* **2001**, *3*, 5459.
- (8) Perdew, J. P.; Savin, A.; Burke, K. *Phys. Rev. A* **1995**, *51*, 4531.
- (9) Fuchs, M.; Niquet, Y.-M.; Gonze, X.; Burke, K. *J. Chem. Phys.* **2005**, *122*, 094116.
- (10) Shao, Y.; Head-Gordon, M.; Krylov, A. I. *J. Chem. Phys.* **2003**, *118*, 4807.
- (11) Mulliken, R. S. *Phys. Rev.* **1932**, *41*, 751.
- (12) Salem, L. *Science* **1976**, *191*, 822–830.
- (13) Bonacic-Koutecky, V.; Bruckmann, P.; Hiberty, P.; Koutecky, J.; Leforestier, C.; Salem, L. *Angew. Chem., Int. Ed. Engl.* **1975**, *14*, 575–576.
- (14) McWeeny, R. *Methods of Molecular Quantum Mechanics*, 2nd ed.; Academic Press: Oxford, U.K., 1992.
- (15) Pople, J. A.; Nesbet, R. K. *J. Chem. Phys.* **1954**, *22*, 571. Berthier, G. *J. Chim. Phys. Biol.* **1954**, *51*, 363.
- (16) Ziegler, T.; Rauk, A.; Baerends, E. J. *Theor. Chim. Acta* **1977**, *43*, 261.
- (17) von Barth, U. *Phys. Rev. A* **1979**, *20*, 1693.
- (18) Frank, I.; Hutter, J.; Marx, D.; Parinello, M. *J. Chem. Phys.* **1998**, *108*, 4060.
- (19) Filatov, M.; Shaik, S. *Chem. Phys. Lett.* **1998**, *288*, 689.
- (20) Filatov, M.; Shaik, S. *J. Chem. Phys.* **1999**, *110*, 116.
- (21) Gräfenstein, J.; Kraka, E.; Cremer, D. *Chem. Phys. Lett.* **1998**, *288*, 593–602.
- (22) Filatov, M.; Shaik, S. *Chem. Phys. Lett.* **1999**, *304*, 429.
- (23) Filatov, M.; Shaik, S. *J. Phys. Chem. A* **2000**, *104*, 6628.
- (24) Cremer, D.; Filatov, M.; Polo, V.; Kraka, E.; Shaik, S. *Int. J. Mol. Sci.* **2002**, *3*, 604.
- (25) Illas, F.; Moreira, I.; de, P. R.; Bofill, J. M.; Filatov, M. *Phys. Rev. B* **2004**, *70*, 132414.
- (26) Illas, F.; Moreira, I.; de, P. R.; Bofill, J. M.; Filatov, M. *Theor. Chem. Acc.* **2006**, *116*, 587–597.
- (27) Moreira, I.; de, P. R.; Costa, R.; Filatov, M.; Illas, F. *J. Chem. Theory Comput.* **2007**, *3*, 764–774.
- (28) Gaudoin, R.; Burke, K. *Phys. Rev. Lett.* **2004**, *93*, 173001; **2005**, *94*, 029901.
- (29) Schautz, F.; Buda, F.; Filippi, C. *J. Chem. Phys.* **2004**, *121*, 5836–5844.
- (30) Buda, F.; Filippi, C. *J. Chem. Phys.* **2005**, *122*, 087102.
- (31) Levy, M.; Nagy, Á. *Phys. Rev. Lett.* **1999**, *83*, 4361–4364. Nagy, Á.; Levy, M. *Phys. Rev. A* **2001**, *63*, 052502.
- (32) Samal, P.; Harbola, M. K.; Holas, A. *Chem. Phys. Lett.* **2006**, *419*, 217–222.
- (33) Samal, P.; Harbola, M. K. *J. Phys. B: At. Mol. Opt. Phys.* **2006**, *39*, 4065–4080.
- (34) Levy, M. *Phys. Rev. A* **1982**, *26*, 1200.
- (35) Lieb, E. H. *Int. J. Quantum Chem.* **1983**, *24*, 243.
- (36) Oliveira, L. N.; Gross, E. K. U.; Kohn, W. *Phys. Rev. A* **1988**, *37*, 282. Gross, E. K. U.; Oliveira, L. N.; Kohn, W. *Phys. Rev. A* **1988**, *37*, 2805, 2809.
- (37) Rajagopal, A. K.; Bout, F. A. *Phys. Rev. A* **1995**, *51*, 1770–1775.
- (38) Salem, L.; Rowland, C. *Angew. Chem., Int. Ed. Engl.* **1972**, *11*, 92–111.
- (39) Cordova, F.; Dorio, J.; Ipatov, A.; Casida, M. E.; Filippi, C.; Vela, A. *J. Chem. Phys.* **2007**, *127*, 164111.
- (40) Baerends, E. J. *Phys. Rev. Lett.* **2001**, *87*, 133004.
- (41) Casida, M. E.; Gutierrez, F.; Guan, J.; Gadea, F.-X.; Salahub, D.; Daudey, J.-P. *J. Chem. Phys.* **2000**, *113*, 7062.
- (42) Gritsenko, O. V.; van Gisbergen, S. J. A.; Görling, A.; Baerends, E. J. *J. Chem. Phys.* **2000**, *113*, 8478.
- (43) Wanko, M.; Garavelli, M.; Bernardi, F.; Niehaus, T. A.; Frauenheim, T.; Elstner, M. *J. Chem. Phys.* **2004**, *120*, 1674.
- (44) Roos, B.; Taylor, P. R. *Chem. Phys.* **1980**, *48*, 157–173.
- (45) Andemson, K.; Malmqvist, P.-Å.; Roos, B.; Andrzej, O.; Sadlej, J.; Wolinski, K. *J. Phys. Chem.* **1990**, *94*, 5483–5488.
- (46) Englisch, H.; Englisch, R. *Phys. Stat. Sol. (B)* **1984**, *123*, 711; *124*, 373.
- (47) Kraka, E.; Gräfenstein, J.; Filatov, M.; Joo, H.; Izotov, D.; Gauss, J.; He, Y.; Wu, A.; Polo, V.; Olsson, L.; Konkoli, Z.; He, Z.; Cremer, D. *COLOGNE08*; University of the Pacific: Stockton, CA, 2008.
- (48) Krishnan, R.; Binkley, J. S.; Seeger, R.; Pople, J. A. *J. Chem. Phys.* **1980**, *72*, 650.
- (49) Stephens, P. J.; Devlin, F. J.; Chabalowski, C. F.; Frisch, M. J. *J. Phys. Chem.* **1994**, *98*, 11623.
- (50) Becke, A. D. *J. Chem. Phys.* **1993**, *98*, 1372.
- (51) Lee, C.; Yang, W.; Parr, R. G. *Phys. Rev. B* **1988**, *37*, 785.
- (52) Karlström, G.; Lindh, R.; Malmqvist, P.-Å.; Roos, B. O.; Ryde, U.; Veryazov, V.; Widmark, P.-O.; Cossi, M.; Schimmelpfennig, B.; Neogrady, P.; Seijo, L. *Comput. Mater. Sci.* **2003**, *28*, 222.
- (53) Zijlstra, R. Excited State Charge Separation in Symmetrical Alkenes. Ph.D. thesis, 2001.
- (54) Groenhof, G. Understanding Light-Induced Conformational Changes in Molecular Systems from First Principles. Ph.D. thesis, 2005.
- (55) Grimm, S. Theoretische Untersuchung von π -Bindungssystemen im Restricted Open Shell Kohn-Sham-Modell. Ph.D. thesis, 2005.
- (56) Grüning, M.; Gritsenko, O. V.; Baerends, E. J. *J. Chem. Phys.* **2003**, *118*, 7183–7192.
- (57) Aryasetiawan, F.; Gunnarsson, O.; Rubio, A. *Europhys. Lett.* **2002**, *57*, 683.
- (58) Coulson, C. A.; Fischer, I. *Philos. Mag.* **1949**, *40*, 386.
- (59) Kolos, W.; Wolniewicz, L. *J. Chem. Phys.* **1965**, *43*, 2429.
- (60) Kolos, W.; Wolniewicz, L. *J. Chem. Phys.* **1966**, *45*, 509.
- (61) Cremer, D. *Mol. Phys.* **2001**, *99*, 1899.
- (62) Polo, V.; Kraka, E.; Cremer, D. *Mol. Phys.* **2002**, *100*, 1771.
- (63) Serrano-Andrés, L.; Merchán, M.; Nebot-Gil, I.; Lindh, R.; Roos, B. O. *J. Chem. Phys.* **1993**, *98*, 3151.
- (64) Douglas, J. E.; Rabinovitch, B. S.; Looney, F. S. *J. Chem. Phys.* **1955**, *23*, 315.
- (65) Foo, P. D.; Innes, K. K. *J. Chem. Phys.* **1974**, *60*, 4582.
- (66) Sension, R. J.; Hudson, B. S. *J. Chem. Phys.* **1989**, *90*, 1377.
- (67) Grimm, S.; Nonnenberg, C.; Frank, I. *J. Chem. Phys.* **2003**, *119*, 11574.
- (68) Haugen, W.; Traetteberg, M. *Acta Chem. Scand.* **1966**, *1726*. Traetteberg, M. *Acta Chem. Scand.* **1968**, *22*, 628.
- (69) Woywod, C.; Livingood, W. C.; Frederick, J. H. *J. Chem. Phys.* **2000**, *112*, 613.
- (70) Leopold, D. G.; Pendley, R. D.; Roebber, J. L.; Hemley, R. J.; Vaida, V. *J. Chem. Phys.* **1984**, *81*, 4218.
- (71) Borden, W. T.; Davidson, E. R. *J. Am. Chem. Soc.* **1977**, *99*, 4587.